Flow around two tubes in an in-line arrangement: flow visualizations and pressure measurements

Ljungkrona, Lars; Norberg, Christoffer; Sundén, Bengt

Published in:
Experimental Heat Transfer, Fluid Mechanics, and Thermodynamics

1991

FLOW AROUND TWO TUBES IN AN IN-LINE ARRANGEMENT; FLOW VISUALIZATIONS AND PRESSURE MEASUREMENTS

Lars Ljungkrona, Christoffer Norberg and Bengt Sunden

Chalmers University of Technology, Department of Thermo- and Fluid Dynamics, 412 96 Göteborg, Sweden

ABSTRACT

An experimental investigation of the flow around and the pressure on two tubes (circular cylinders) rigidly mounted in an in-line or tandem arrangement has been carried out.

Flow visualizations were performed in a subcritical Reynolds number range, $3300 \leq Re \leq 12000$ for dimensionless tube spacings in the range of $1.25 \leq S/D \leq 4.0$, using a smoke wire technique.

The fluctuating wall pressures were recorded by a microphone in a pinhole arrangement. The Reynolds number was Re = 20000, and three different turbulence intensities of the approaching cross-flow (0.1 %, 1.4 % and 3.2 %) were considered. The spacing between the tubes was in the range of $1.25 \leq S/D \leq 5.0$.

The flow visualizations and the pressure measurements clearly revealed that the flow depends on the Reynolds number, freestream turbulence intensity and tube spacing.

INTRODUCTION

The flow around two tubes in an in-line or tandem arrangement is of engineering interest since various constructions include this geometry. The interference between the two tubes results in a flow that can be divided in different flow regimes. The occurrence of these flow regimes is strongly dependent of the freestream conditions, the Reynolds number Re, turbulence intensity Tu, length scale of turbulence Λ, the spacing between the tubes S, the aspect ratio of the tubes L/D, if end plates are used or not, roughness of tube surface, etc. Fig. 1 provides a sketch of an in-line arrangement with the nomenclature adapted in this work.

Many authors have dealt with different aspects of the flow around the tubes. Zdravkovich [1,2] have classified the flow in different regimes. Igarashi [3] studied the pressure fluctuations on the tubes and carried out flow visualizations in order to classify the flow. Huhe-Aode *et al.* [4] performed flow visualizations to investigate the wake structure at very low Reynolds numbers. Nishimura *et al.* [5] presented flow visualizations and mass transfer experiments to reveal how the heat transfer on the tubes depends on the flow field.

The classifications due to Igarashi and Zdravkovich for a non-turbulent freestream are very similar. The interference between the two

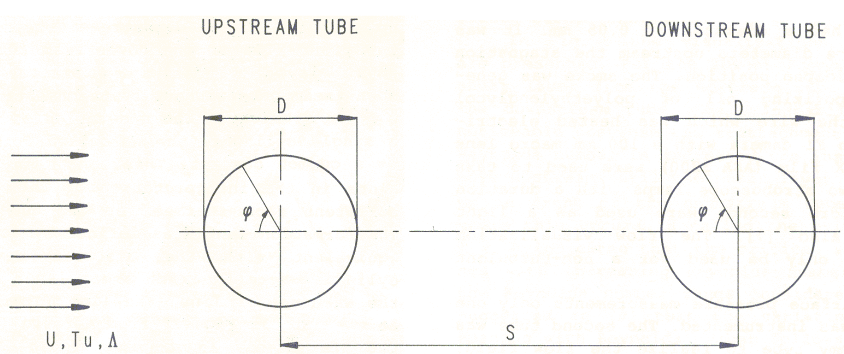

Fig. 1. Two tubes in a tandem arrangement.

Experimental Heat Transfer, Fluid Mechanics, and Thermodynamics 1991
J.F. Keffer, R.K. Shah, and E.N. Ganić, Editors

tubes is called wake interference when one tube is submerged in the wake of the other [1]. For $1 \le S/D \le 1.2 - 1.8$ the free shear layer separated from the upstream tube does not reattach on the downstream tube. The vortex street behind the latter is formed by the shear layer from the former. When $1.2 - 1.8 \le S/D \le 3.4 - 3.8$, the shear layer from the upstream tube reattaches on the downstream tube. A vortex street is formed behind the downstream tube. For $3.4 - 3.8 \le S/D \le 6.0$, the separated boundary layer from the upstream tube rolls up and forms vortices in front of the downstream tube. The spacing at which this phenomena starts to occur is called the critical spacing. Above S/D = 6.0 a new vortex street is found to be independently shed from the downstream tube [6]. The classification above is valid at least in the range Re = 10000 - 380000.

In the present investigation flow visualizations are presented together with pressure measurements in order to show how variations in the pressure fluctuations are related to the different flow regimes occurring.

EXPERIMENTAL ARRANGEMENT AND INSTRUMENTATION

All experiments were carried out in a closed-circuit, low-speed wind tunnel. The working section is rectangular with a height of 0.5 m and a width of 0.4 m. The streamwise turbulence intensity in the working section is less than 0.1 %. The r.m.s. pressure coefficient of the acoustic field in the working section is less than 2 % at the freestream velocity used in the pressure measurements, 15 m/s.

In both the flow visualizations and the pressure measurements, two smooth tubes with a diameter of 20 mm and with end plates were rigidly mounted in the wind tunnel walls. The aspect ratio of the tubes was 15.8, and the total blockage of the working section, including the end plates, was 6.3 %.

The smoke wire technique was used to visualize the flow field. The smoke wire was made of nichrome and had a diameter of 0.05 mm. It was placed 1.5 tube diameters upstream the stagnation line at the midspan position. The smoke was generated by vaporizing oil of polyethylenglycol supplied to the wire which was heated electrically. A Canon F1 camera with a 100 mm macro lens and Kodak TMAX film (ASA 3200) were used to take the photos. Two stroboscope lamps with a duration time of 5 micro seconds were used as a light source, see also [7]. The flow visualization technique can only be used for a non-turbulent freestream.

In the surface pressure measurements only one of the tubes was instrumented. The second tube was used as a dummy tube to realize the flow field. The tubes were shifted between the upstream and downstream positions to enable measurements at both locations. The instrumented tube was fitted with a 1/4" microphone, B & K Type 4135, for measurement of the fluctuating pressure. The microphone was mounted in a pinhole arrangement. A linear frequency response (within $\pm$ 3 dB) was achieved between 3 - 1000 Hz. A separate pressure tap connected to a micromanometer, Furness FCO 14, was used to measure the mean pressure. The separation between the static pressure tap and the tap for the fluctuating pressure was 18 mm. The uncertainty in the r.m.s. pressure coefficient was estimated to be less than 3 % and in the mean pressure coefficient less than 1 %. The estimations of the uncertainties follow the principals outlined by Moffat [8].

The technique described for measuring the wall pressure field is thoroughly described in [9].

RESULTS AND DISCUSSION

The flow visualizations were carried out at four different Reynolds numbers 3300, 6700, 10000 and 12000, for the dimensionless spacing between the tubes, S/D = 1.25, 1.5, 2.0, 3.0 and 4.0.

The pressure measurements were mainly carried out at Re = 20000 with three different turbulence intensities of the approaching cross flow (Tu = 0.1 %, 1.4 % and 3.2 %). The spacing between the tubes was S/D = 1.25, 1.5, 2.0, 2.5, 3.0, 3.5, 4.0 and 5.0.

Since the Reynolds numbers for the flow visualizations and that of the pressure measurements do not coincide, a comparison between the two types of experiments is not straigth forward. The results of the flow visualizations are mainly used to support the findings of the wall pressure measurements.

Formation length

The flow around the tubes is much affected by the behavior of the separated boundary layer from the upstream tube. The different flow regimes involved depend on whether this shear layer rolls up in front of the downstream tube, reattaches on the front side of the downstream tube, or if the shear layer is forming vortices behind the downstream tube without reattachment.

In studies of the generation of vortices from a single cylinder, the so-called formation length is a common concept. This length may provide some hints in the interpretation of the occurrence of different flow regimes for two tubes in tandem. The formation length as defined by Gerrard [10] is equivalent with the distance downstream the cylinder where the free shear layer first crosses the wake center line (the line normal to the tube at $\varphi = 180^\circ$). Fig. 2, from Norberg [11], provides the formation length as found by different authors. It is obvious that the formation length is strongly dependent on the Reynolds number. Later, Fig. 2 will be referred to.

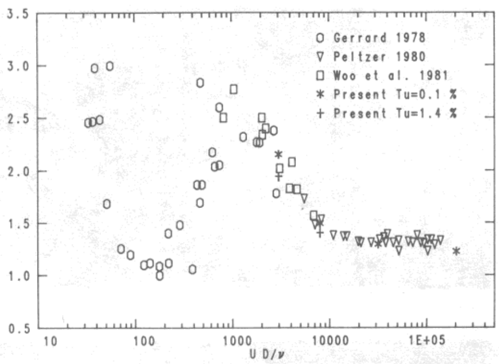

Fig. 2. Vortex formation length versus Reynolds number, from [10].

Flow visualizations

The flow visualizations for the smallest spacing, S/D = 1.25, are presented in Fig. 4. For the lowest Reynolds number, Re = 3300, the vortices formed behind the downstream tube seem to be quite large and stretches the streamlines in the entrained flow considerably, see Fig. 4a. This implies that the flow is rather violent. The separated boundary layer from the upstream tube form vortices behind the downstream tube, without reattachment on the downstream tube. Fig. 2 shows that the formation length is about 2 diameters at this Reynolds number which is large enough for the shear layer to form vortices behind the downstream tube without reattachment, and the two tubes may be regarded as a single body. This is supported by the flow visualization for a single cylinder at Re = 3000, provided in Fig. 3. If this flow is

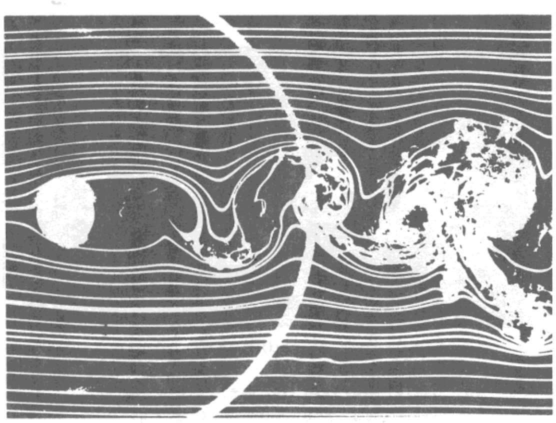

Fig. 3. Visualization of single cylinder at Re = 3000.

compared to that obtained at Re = 3300 for the in-line arrangement at S/D = 1.25, Fig. 4a, one notices that the wake structure and formation of vortices look very similar. Hence for flows with large formation lengths the formation of vortices do not seem to be influenced by the presence of a downstream tube with equal diameter. As the Reynolds number is increased the formation length decreases according to Fig. 2. This implies that the downstream tube will block the formation of vortices more efficiently since there is less space for the vortices to form freely. This is seen in Fig. 4a-d as a decrease in size of the vortices behind the downstream tube, resulting in a more narrow wake, as the Reynolds number is increased. The entrained flow is also less stretched for the higher Reynolds numbers indicating a less violent flow.

The visualizations showed that the flow for S/D = 1.5 is very similar to that at S/D = 1.25 showing no reattachment of the shear layer on the downstream tube. Also at this spacing the flow seems to become less violent with increasing Reynolds number.

As the spacing between the tubes is increased to S/D = 2.0, there is still no reattachment onto the downstream tube for the lowest Reynolds number, see Fig. 5a. The formed vortices are large in size with strong stretching of the entrained flow. When the Reynolds number increases to Re = 6700 the formation of vortices is blocked and the shear layer reattaches on the downstream tube. This results in smaller vortices behind the downstream tube. The vortex street behind this tube is formed as the reattached shear layer separates from it. The wake flow for the cases with no reattachment, see Fig. 4 and 5a seems to be more violent than the cases with reattachment, Fig. 5b-d. This is a reflection of the different flow mechanisms involved in the two flow regimes.

For S/D = 3.0 and the lowest Reynolds number the shear layer reattaches on the downstream tube and the vortex street behind the tubes is weak. As the Reynolds number increases the intensity of the vortex street increases.

In Fig. 6 the visualizations for S/D = 4.0 are presented. For the lowest Reynolds number the shear layer from the upstream tube reattaches on the downstream tube. Small instability waves are noticeable upstream the reattachment point. As the Reynolds number is increased the instability waves move upstream until the shear layer starts to roll up in front of the downstream tube. The spacing where this occurs is called the critical spacing. Fig. 6 indicates that the critical spacing decreases with increasing Reynolds number at least in the Reynolds number range considered here. It is suggested in [9] that the variation in critical spacing with Reynolds number follows the variation in the formation length for a non-turbulent free-stream.

The effects of increased tube spacing are clearly seen for the highest Reynolds number,

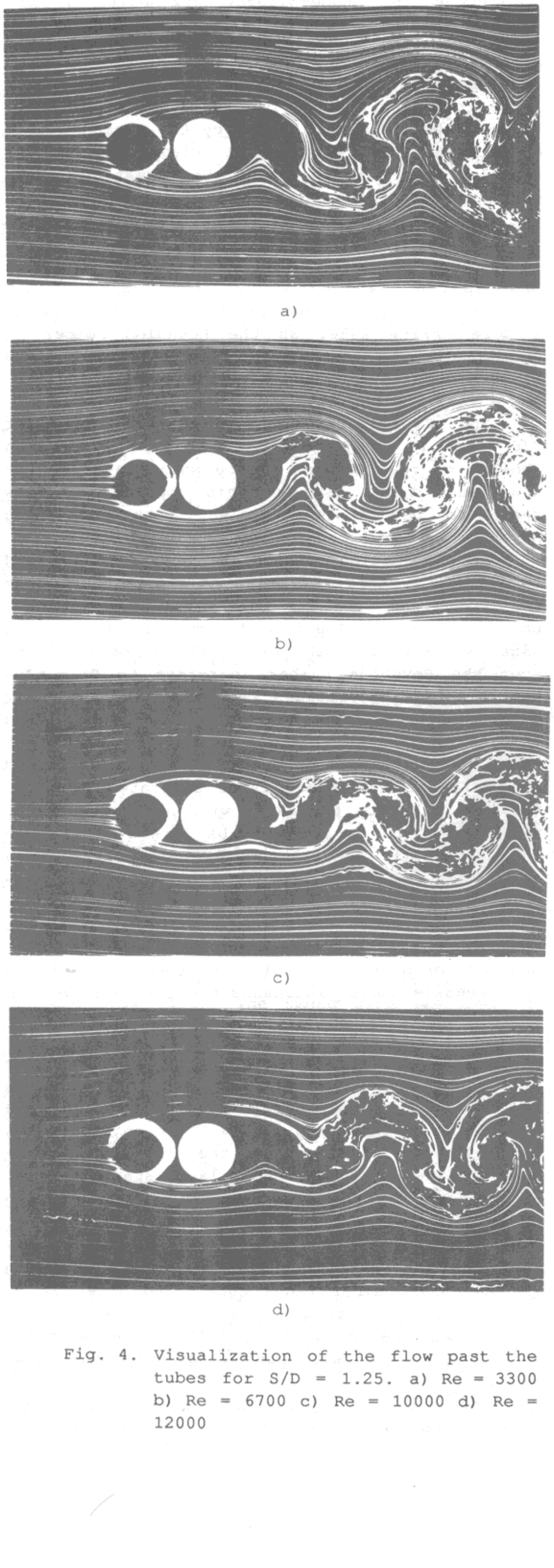

Fig. 4. Visualization of the flow past the tubes for S/D = 1.25. a) Re = 3300 b) Re = 6700 c) Re = 10000 d) Re = 12000

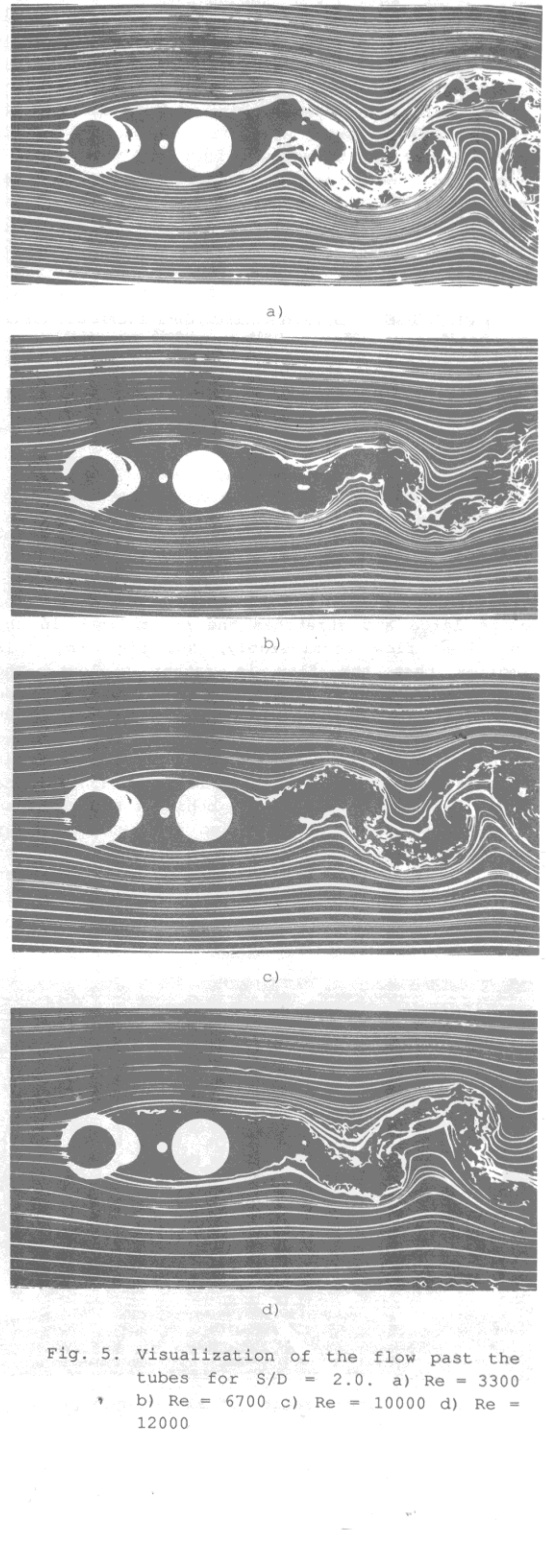

Fig. 5. Visualization of the flow past the tubes for S/D = 2.0. a) Re = 3300 b) Re = 6700 c) Re = 10000 d) Re = 12000

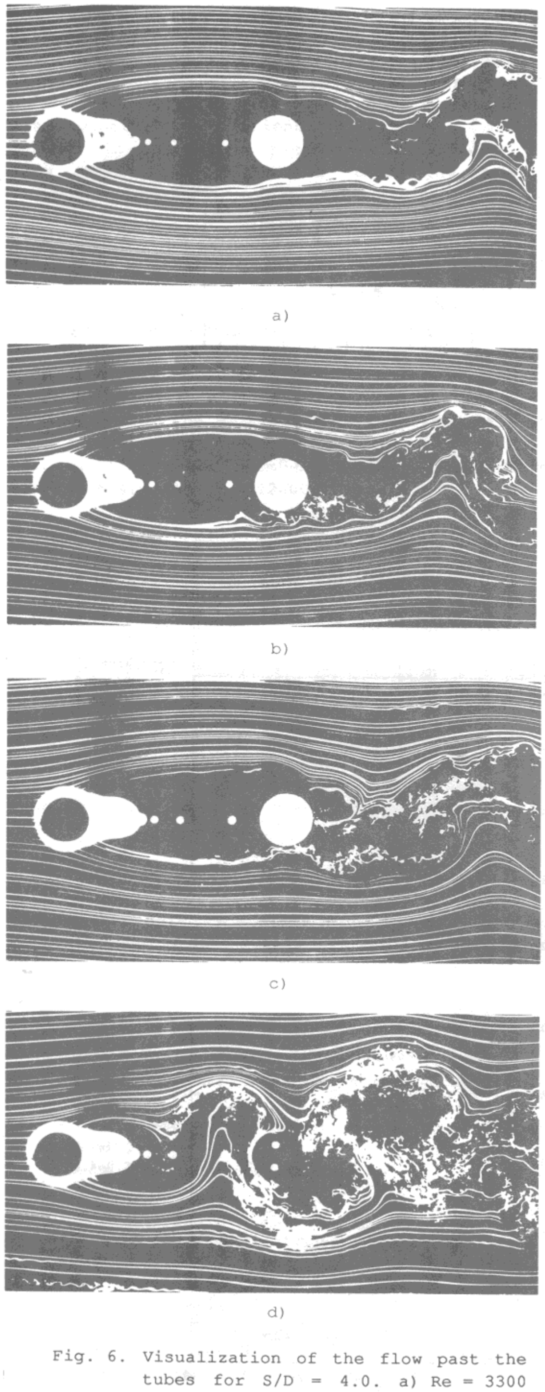

a)

b)

c)

d)

Fig. 6. Visualization of the flow past the tubes for S/D = 4.0. a) Re = 3300 b) Re = 6700 c) Re = 10000 d) Re = 12000

Re = 12000, Fig. 4d, 5d and 6d. At this Reynolds number all flow regimes are present as pointed out by Zdravkovich [1]. At S/D = 1.25 the two tubes can be seen as a single body since the separated boundary layer from the upstream tube does not reattach on the downstream tube. When the tube spacing is increased to S/D = 2.0 the shear layer reattaches on the front side of the downstream tube and separates at the rear part of that tube. The shedding from the downstream tube seems to be quite weak and the wake is rather narrow. At S/D = 4.0 the critical spacing is exceeded and the shear layer rolls up in front of the downstream tube. The vortex shedding from the tubes is synchronized and strong vortices are formed behind the downstream tube.

Pressure measurements

The visualizations showed that there are large variations in the flow field as the spacing between the tubes and Reynolds number are changed. Such variations in the flow field must also be reflected in the wall pressure around the tubes.

Fig. 7 provides the mean drag coefficient, C_D, and the Strouhal number, Sr, as function of the tube spacing, S/D. The critical spacing is clearly seen in Fig. 7 as a discontinuous increase in C_D and Sr at S/D = 3.5 for the non-turbulent case. By introducing turbulence in the freestream, the critical spacing decreases considerably as is shown in C_D on the downstream tube. For the turbulent cases, a discontinuous change does not appear in C_D on the upstream tube or in the Strouhal number.

The mean and r.m.s. pressure coefficients on the upstream and downstream tubes for the non-turbulent case are provided in Fig. 8 and 9, respectively. The mean pressure coefficient on the upstream tube is similar to that obtained on a single cylinder for all spacings. The difference is mainly in the base pressure.

At S/D = 1.25 and 1.5 the mean pressure coefficient on the downstream tube is characterized by a maximum at the point of reattachment, $\varphi \approx 80^\circ$. There is also a maximum in the r.m.s. pressure coefficient at $\varphi \approx 70^\circ$ due to reattachment. The generally low levels in the r.m.s. pressure coefficient and the high Strouhal numbers, Sr = 0.24 and 0.23 indicates a flow with weak vortex shedding. This is supported by the flow visualizations for S/D = 1.25 and 1.5, where the vortex shedding was suppressed more with increasing Reynolds number due to a decrease in formation length. For the turbulent cases, there is a large decrease in Strouhal number for S/D = 1.25 and 1.5. This change is due to a transition to a flow with stronger vortex shedding. The flow is what Igarashi [3] calls synchronized vortex shedding and is established at Reynolds numbers above Re = 35000. For more details, see [9].

For the cases with reattachment and vortex shedding from the downstream tube, S/D = 2.0 -3.0,

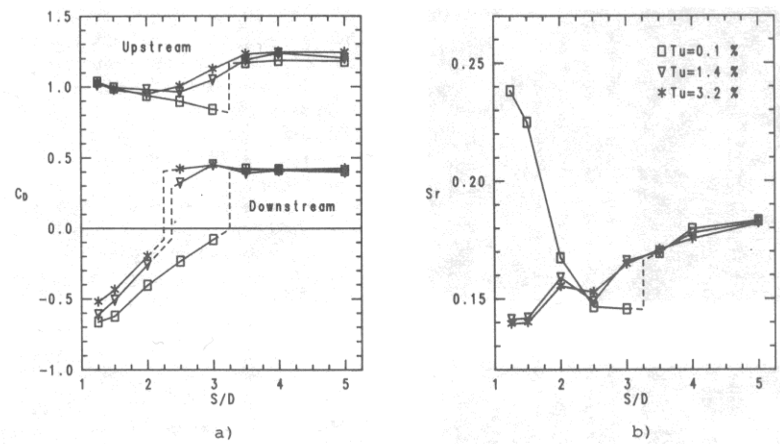

Fig. 7. Variation of a) drag coefficient and b) Strouhal number with tube spacing.

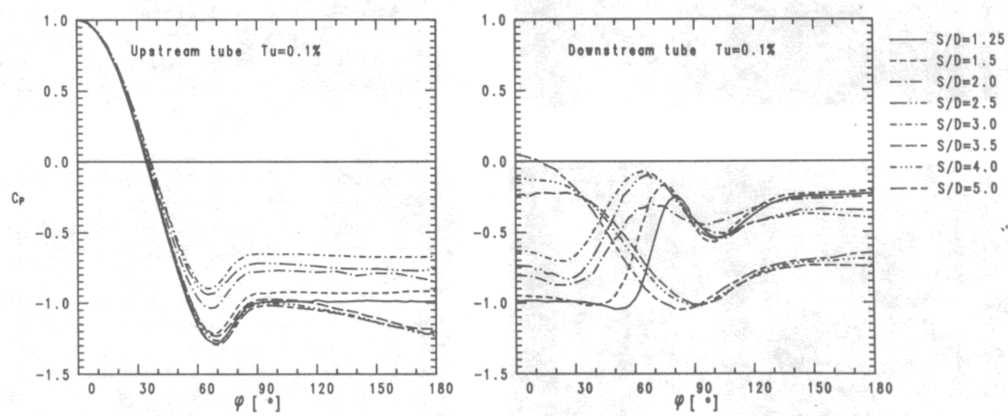

Fig. 8. Mean pressure distribution around the tubes for a non-turbulent freestream.

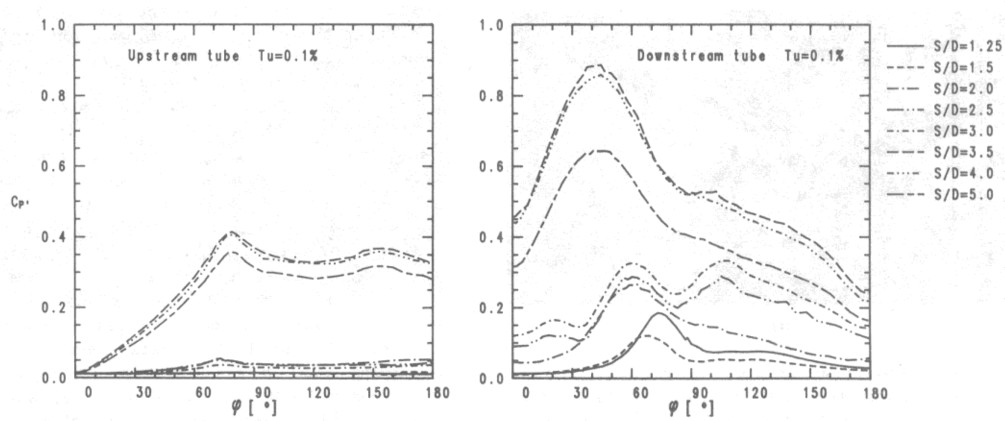

Fig. 9. R.m.s. pressure distribution around the tubes for a non-turbulent freestream.

the Strouhal number decreases and the r.m.s pressure coefficient increases compared to S/D = 1.25 and 1.5. This indicates a stronger vortex shedding than at the smaller spacings. The reattachment point is clearly observed as a flat maximum in the mean pressure coefficient at $\varphi \approx 70^\circ$ and at $\varphi \approx 60^\circ$ in the r.m.s. pressure coefficient. The flow visualizations showed that the vortex strength increases, for S/D = 3.0, when the Reynolds number is increased to 12000. It is likely that the strength of the vortex shedding will increase further as the Reynolds number is increased to Re = 20000.

At spacings above the critical, $S/D \geq 3.5$, the mean pressure distribution is similar to that for high Reynolds numbers with a delayed separation at $\varphi \approx 120^\circ$. There is a pronounced maximum in the r.m.s. pressure coefficient at $\varphi \approx 45^\circ$ due to impingement of the vortices shed from the upstream tube on the front side of the downstream tube. This is also clear from the flow visualizations for S/D = 4.0 and Re = 12000, Fig. 6d.

CONCLUSIONS

The flow visualizations show that the flow around the tubes is affected by both Reynolds number and tube spacing.

The vortex formation length from a single cylinder may be used to explain the Reynolds number dependence of the occurrence of the different flow regimes around the tubes.

The alterations in the flow pattern are significantly reflected in the pressure distributions on the tubes and the Strouhal number.

ACKNOWLEDGEMENT

The present work is financially supported by the National Swedish Board for Technical Development (STU).

NOMENCLATURE

C_D mean drag coefficient $\int C_p \cos\varphi \, d\varphi$, dimensionless
C_p mean pressure coefficient $((p-p_\infty)/q)$, dimensionless
$C_{p'}$ r.m.s. pressure coefficient (p'_{rms}/q), dimensionless
D tube diameter, m
f_s shedding frequency (Strouhal frequency), Hz
L tube length, m
p mean pressure on tube surface, Pa
p_∞ reference pressure (static pressure from a Pitot static tube placed 0.5 m upstream the tubes), Pa
p′ fluctuating surface pressure, Pa
p'_{rms} r.m.s of pressure fluctuations, Pa
q dynamic pressure $(\rho U^2/2)$, Pa
Re Reynolds number (UD/ν), dimensionless
S spacing between the tubes, m
Sr Strouhal number $(f_s D/U)$, dimensionless
Tu turbulence intensity (u'_{rms}/U), dimensionless
u'_{rms} r.m.s. of streamwise fluctuating velocity, m/s
U freestream velocity, m/s

ν kinematic viscosity of the fluid, m^2/s
ρ density, kg/m^3
φ angle from stagnation point, degrees
Λ integral length scale of streamwise fluctuating velocity, m

REFERENCES

1. Zdravkovich, M.M., The effects of interference between circular cylinders in cross flow, J. Fluids and Structure, 1, 239-261, 1987.

2. Zdravkovich, M.M., Rewiew of flow interference between two circular cylinders in various arrangements, J. Fluids Eng., Vol. 99, No. 4, 618-633, 1977.

3. Igarashi, T., Characteristics of the flow around two circular cylinders arranged in tandem. 1st Report. Bull. JSME, Ser. B, Vol. 24, No. 118, 323-331, 1981.

4. Huhe-Aode, Tatsuno, M. and Taneda, S., Visual studies of wake structure behind two cylinders in tandem arrangement, Reports of Research Inst. Appl. Mech., Kyushu Univ., Japan, Vol. XXXII, No. 99, 1-20, 1985.

5. Nishimura, T., Ohori, Y., and Kawamura, Y., Flow pattern and rate of mass transfer around two cylinders in tandem, Int. Chem. Eng., Vol. 26, No. 1, 123-129, 1986.

6. Ohya, Y., Okajima, A. and Hayashi, M., Wake interference and vortex shedding, Encyc. Fluid Mechanics, Vol. 8, 322-389, Gulf Publishing Company, 1989.

7. Jauhianen, A. and Norberg, C., Visualizations using a combined unit for the smoke wire and hydrogen bubble technique, Report, Nr 89/16, Dept. Appl. Thermod. and Fluid Mech., Chalmers Univ. of Tech., Gothenburg, Sweden, 1989, (In Swedish).

8. Moffat, R.J., Describing uncertainties in experimental results, Experimental Thermal and Fluids Science, 1, 3-17, 1988.

9. Ljungkrona, L., Influence of freestream turbulence and tube spacing on wall pressures for two tubes in an in-line arrangement, Thesis for the Degree of Licentiate of Eng., Dept. Appl. Thermod. and Fluid Mech., Chalmers Univ.

of Tech., Gothenburg, Sweden, paper I, 1-48, 1989.

10. Gerrard, J.K., The wakes of cylindrical bluff bodies at low Reynolds number, Phil. Trans. Roy. Soc., London, Ser. A, Vol. 288, No. 1354, 351-382, 1978.

11. Norberg, C., Reynolds number and freestream turbulence effects on the flow and fluid forces for a circular cylinder in cross flow, Ph.D., Thesis Dept. Appl. Thermod. and Fluid Mech., Chalmers Univ. of Tech., Gothenburg, Sweden, paper IV, 1-50, 1987.